Int J Adv Manuf Technol (2017) 91:3551–3559
DOI 10.1007/s00170-017-0009-7

ORIGINAL ARTICLE

# Numerical-experimental investigation on the rabbit ear formation mechanism in gear rolling

**Jin Li**[1] · **Guangchun Wang**[1] · **Tao Wu**[1]

Received: 9 August 2016 / Accepted: 4 January 2017 / Published online: 25 January 2017


**Abstract** The formation of rabbit ears during the gear rolling process, caused by the generating motion between the gear roller and the blank, is a common and undesirable phenomenon encountered in gear rolling. It generally leads to fold defects, waste of material, and decline in mechanical properties after removal, seriously affecting the quality of the gear to be formed. In this paper, a finite element model of gear rolling is first established, the gear rolling process are simulated, and the rabbit ear formation mechanism and its morphology change are studied. The phenomenon and the morphology of the rabbit ear are then verified experimentally. The formation mechanism of the rabbit ear was analyzed by means of the stress state, the deformation distribution, and the material flow. The results show the following: (1) the continuous localized contact between the gear roller and the blank induces the material on the surface area of the tooth sequential plastic deformation, while at the same time, the material is squeezed by the tooth flank of the gear roller and flows towards the direction of the smaller resistance, that is, the flank of the tooth. The difference in the material flow velocity between the flank of the tooth and the center of the tooth leads to the formation of the rabbit ear; (2) the asymmetric shape of the ears appears to be related to the different direction of friction exerted on two sides of the tooth depending on the rotational direction of the gear roller. These findings provide a scientific basis to further explore measures to control the rabbit ear defect and improve the forming quality in gear rolling.

**Keywords** Gear rolling · Rabbit ear · Formation mechanism · Finite element analysis

## 1 Introduction

Gears are widely used as mechanical driving devices in power transmission systems. At present, cutting is the main method to manufacture gears. Owing to the high utilization ratio of materials, as well as the high mechanical properties of the parts, the plastic forming process has become increasingly important in gear production. Since the 1960s, scholars from different countries have carried out research on gear forging, put forward a variety of process methods to reduce the deformation resistance, and tried to apply them to practical production [1–4]. However, in the course of gear forging replacing gear cutting, the tooth surface precision has decreased and the unmolding becomes difficult due to large elastic deformation, and the work condition is thus poor due to the larger load.

Targeting the abovementioned problems of gear forging, combined to the advantage of rolling and referring to the process principle of thread rolling, the gear rolling process has been put forward. The forming principle of gear rolling is shown in Fig. 1, a pair (or more) of gear rollers with the same parameters are installed in parallel in their respective shaft, and they rotate synchronously in the same direction driven by the transmission mechanism and extrude the blank along the radial axis simultaneously. The material of the outer part of the blank gradually forms the tooth shape through the generating motion with the gear roller [5]. In the middle stage of gear rolling, due to the increase of feed of the gear roller, sharp protrusions appear and gradually grow larger on both sides of

✉ Guangchun Wang
wgc@sdu.edu.cn

[1] Key Laboratory for Liquid-Solid Structural Evolution and Processing of Materials, Shandong University, Jingshi Road , 17923, Jinan 250061, People's Republic of China

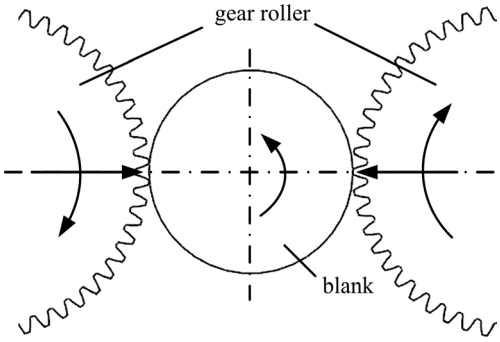


**Fig. 1** Schematic diagram of gear rolling

each tooth top. This defect is often called the rabbit ear due to its shape. This is illustrated in Fig. 2. The rabbit ear is prone to fold in the later stage of gear rolling. Even if there are no folding defects, the rabbit ear needs to be removed which leads to waste of materials and increase in working hour; meanwhile, the cutting tends to decrease the mechanical properties of the gear.

Some scholars have carried out relevant research on the rabbit ear in gear rolling. Zheng and Chenthe protrusion on both sides of the top tooth and concave on the center of the top tooth while introducing the research status of gear rolling was mentioned. They pointed out that the flow speed difference between the material of the tooth surface and the material of the core caused this phenomenon and it is concluded that the size of the protrusion is inversely proportional to the bite depth of the gear roller and proportional to the rotation speed of the blank [6]. This paper only refers to the phenomenon and the factors related to the ear rabbit defect but did not conduct a theoretical analysis or an experimental study. Liu and Sun mentioned the rabbit ear defect in their doctoral dissertation, but did not analyze its causes and did not put forward a solution [7, 8]. Wu analyzed forming defects of spline rolling and pointed out that the serious concave on the center of the top tooth was due to high allowance of the blank before rolling, and the solution was to reduce it before rolling [9]. Wang et al. demonstrated that the reason of the size error of the gear to be formed is the metal protrusion in the driven side of the tooth. In the paper, they analyzed the size error of the diameter of small modulus involute spline before rolling, and pointed out incidentally the reason of protrusions on the driven side of the tooth. When the gear roller and the blank meshed, a different relative sliding on two sides of the tooth generated. This made the metal on the driven side flow outwards of the pitch circle and the metal on the active side flow towards the pitch circle, resulting in protrusion on the driven side of the tooth [10]. Zhu et al. analyzed the change of the relative friction direction exerted on two sides of the tooth, and the influence on the flow direction of the metal, through theoretical analysis, numerical simulations, and experiments. They verified that, in the later stage of gear rolling, metal on the active side flows towards the pitch circle, and metal on the driven side flows outwards of the pitch circle, thus confirming that the metal protrusion on the driven side was consistent with the friction direction [11]. Wang and Li proposed a method of adding cylindrical wheel to suppress or eliminate the rabbit ear defects in gear rolling process [12]. Kamouneh et al. simulated gear rolling process and tried to eliminate the rabbit ear by several die stroke combinations. This was the best result by halting the gear roller at 70% of the stroke and then reversing the rolling direction for the remainder of the stroke. The tooth profile of the blank obtained in their simulations is depicted in Fig. 3. Figure 3a shows the tooth profile of the blank without reverse rolling. Figure 3b depicts the tooth profile of the blank with reverse rolling [13]. Through this comparison, it may be seen that the rabbit ear defect is more symmetrical when reverse rolling is utilized (Fig. 3b), but that the size of the ear does not decrease. Therefore, reversing the gear roller does not seem as an effective method to eliminate the rabbit ear defect.

Neugebauer et al. described the gear rolling process. In contrast to flat rolling tools, round tools for helical gears need additional kinematic compensation during diameter-related variable pitch forming processes. The new method shows up to a 50% improvement in pitch accuracy [14, 15]. Neugebauer et al. described the interactions during gear rolling in order to get a method for the prognosis of the attainable quality [16]. Nagata and Kurita invented a gear rolling process with a gear roller of bigger pressure angle; in this process, the gear roller can easily penetrate the blank in the initial stage. This can provide guidance for the later gear rolling [17]. Sasaki et al. optimized the surface rolling process of sintered steel helical gears by using a newly developed CNC form rolling machine, and the feasibility of the new special rolling machine to obtain high-precision helical gears was revealed through an experimental study [18]. Uematsu studied the effect of the variation of angular velocity in gear rolling process on profile error. Although papers and patents about the gear rolling process have been published, some of which mentioned the rabbit ear defect; however, no relevant studies have been reported on the rabbit ear formation and an in-depth analysis on its causes [19].

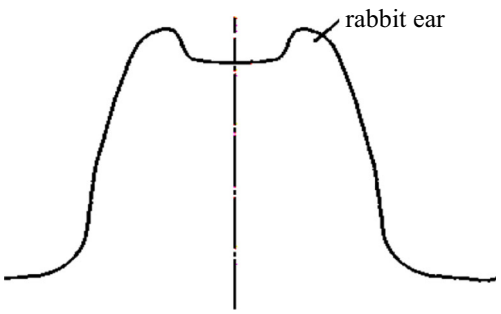


**Fig. 2** Rabbit ear defect

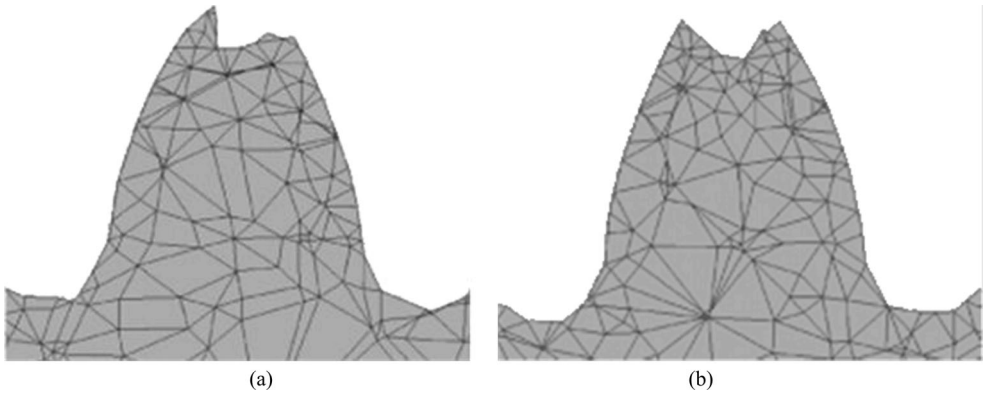

**Fig. 3** Rabbit ear solution. **a** Deform simulation of gear rolling. **b** Deform reverse roll 30% of the stroke

In this paper, a finite element model of gear rolling is established by means of Deform-3D. The phenomenon of the rabbit ear in gear rolling is analyzed by the numerical simulations, which are then confirmed by an experimental study. The formation mechanism of the rabbit ear in gear rolling is described through the force, deformation, and flow analysis.

## 2 Finite element model of gear rolling

Deform-3D software was used to simulate the forming process in gear rolling. The basic parameters and environmental variables of the model are shown in Table 1. Specific settings used were as follows: the gear to be formed and the gear rollers were standard, both the modulus were 1, and both the pressure angles were set as 20°. A shearing friction model was selected. The thickness of the blank was 2 mm; because the deformation along the axis is symmetrical, in order to improve the simulation efficiency, only half thickness was considered with the appropriate symmetry constraint. Because the deformation is mainly concentrated in the annular region of the blank's outer circle and the blank deformation is center symmetric, in order to improve the simulation efficiency, a semi-annular with the radial thickness of 7 mm is simulated, and the two end faces of the half ring are set with symmetry constraints. The main deformation areas, that is, the 2.5-mm0thick annular region of the blank's outer ring, were refined with a mesh density ratio 0.01. The two gear rollers were assumed to be rigid, rotating in the same direction and feeding along the radial direction. The gear roller drives the blank rotate, assuming there is no slipping, so it can be simplified that the blank fixed, the gear rollers rotated and revolved around the blank's center. The angular velocity of the revolution is 18 rpm; the radial feed speed of the gear roller is 0.10 mm/s. Their geometric relations are shown in Fig. 4.

## 3 Simulation results of the gear rolling process

The simulation results are represented in Fig. 5 in terms of the mesh deformation at different stages of the forming process. As shown in Fig. 5, with the increase of the feed of the gear roller, the morphology of the rabbit ear changes. It can be seen from Fig. 5a that when the feed of the gear roller is relatively small, the shape of the tooth top remains flat. Along with the increase of the feed, protrusions on both sides of the tooth top appear, and constantly grow taller (Fig. 5b–d ). When the feed of the gear roller reaches 0.90 mm, the shape of the rabbit ear becomes quite obvious (Fig. 5c), and when the feed reaches 1.10 mm, the right ear is shown to be significantly pulled up and sharp (Fig. 5d). In the later stage of the gear rolling process, with the continual increase of the feed, the teeth of the blank continue to grow taller, the two ears on both sides of the tooth top are squeezed to gather towards the center and a fold defect appears between the two ears. These fold defects are generally expressed by means of the folding angle and are shown in Fig.6, where the maximum folding angle corresponds to 351 degrees. This value is greater than the so-called danger value of 270 degrees [20]. Meanwhile, the teeth of the blank bend towards one side; this is related to the rotation direction of the gear roller. The gear roller revolves

**Table 1** Basic parameters of gear rolling in FEM model

| Basic parameters | Number of teeth on the gear to be formed | Number of teeth on the gear roller | Friction factor | Blank material | Forming temperature(°C) | Blank grid |
|---|---|---|---|---|---|---|
| Value | 31 | 51 | 0.1 | AL_2017 | 20 | 100,000 |

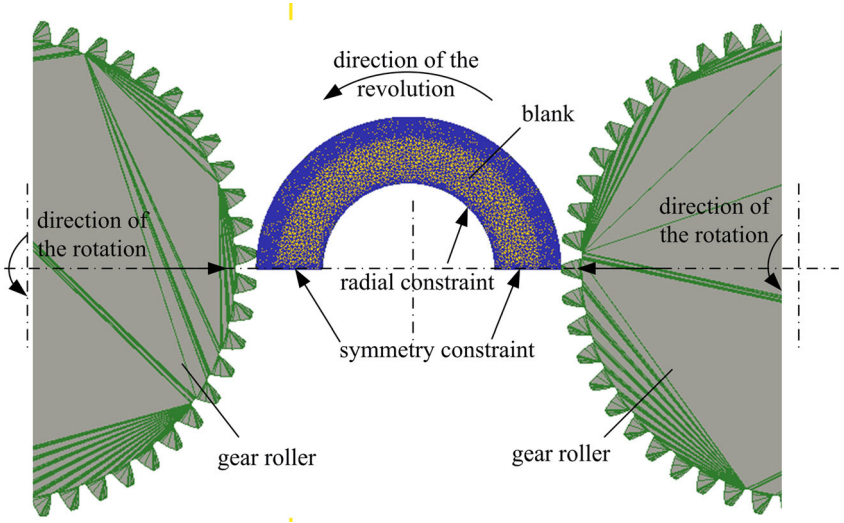


**Fig. 4** Finite element simulation model

counterclockwise around the blank; when one tooth of the blank is formed by the gear roller, the tooth biting into the blank, and the tooth sliding out from the blank on the gear roller generate an torque on this tooth of the blank, it will cause the tooth of the blank bend counterclockwise.

## 4 Analysis of the formation mechanism of the rabbit ear

### 4.1 Force analysis

In the gear rolling process, with the increase of the radial feed of the gear roller, the teeth of the gear roller bite deeper into the blank. The gear roller rotates couterclockwise to drive the blank to rotate clockwise. As shown in Fig.7, tooth *B* gradually bites into tooth *C*, and tooth *A* gradually slides out of tooth *C*. In the course, they roll tooth *C* altogether. The direction of the driving force that tooth *B* exerts on tooth *C* is the same as the rotation direction of the blank, so the contact surface is called the active side; the contact side between tooth *A* and tooth *C* is referred as the driven side.

Tooth *A* first contacts the driven side of tooth *C*, as shown in Fig.7a. Since the gear roller feeds along the radial axis and extrudes the blank simultaneously, tooth *A* exerts pressure *N* on tooth root located on the right side of tooth *C*, and the compressed metal is caused to flow downward and towards both sides. Meanwhile, there is continuous localized contact between tooth *A* and the right side of tooth *C*, and the forces applied on tooth *C* by tooth *A* are as follows: a normal force $N_{AC}$ on the direction perpendicular to the contact surface and a tangential frictional force $f_{AC}$ along the contact surface, direction towards the circle center of the blank. With the continual rotation of the gear roller, tooth *B* contacts the active side of tooth *C*, as shown in Fig.7b, and since tooth *A* gradually slides out of the tooth root, the pressure $N_{AC}$ gradually decreases to 0. At the same time, the generating motion between the right side of tooth *C* and tooth *A* is about to end, and the direction of the friction $f_{AC}$ changes, direction to the tooth top of the blank along the tooth side. At this point, the generating motion between the left side of tooth *C* and tooth *B* has just started, and the forces that tooth *B* exerts on tooth *C* are the normal force $N_{BC}$ and the frictional force $f_{BC}$.

As can be seen from the force analysis above, the gear roller contacts the driven side and the active side of the blank

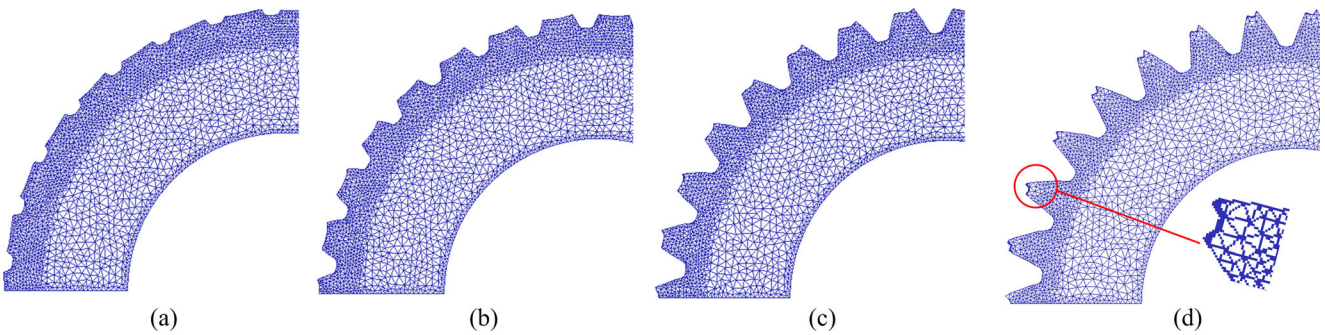


**Fig. 5** The changes of the rabbit ear's morphology in different feed. **a** 0.30 mm. **b** 0.60 mm. **c** 0.90 mm. **d** 1.10 mm

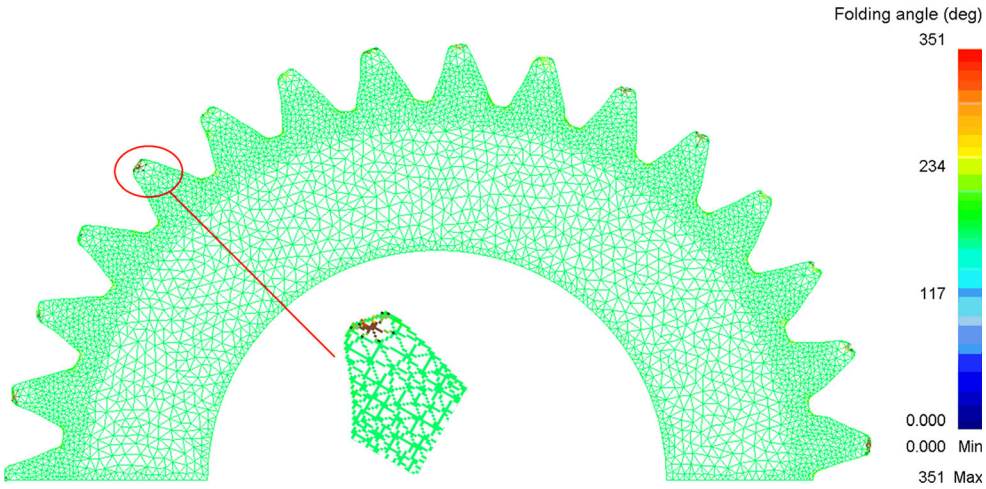


**Fig. 6** Folding defect of the tooth

tooth sequentially, and the generating motion of the driven side and the active side is completed in turn. The pressure *N* exerted on the tooth root of the blank by the tooth of the gear roller is the driving force and lets the metal flow towards the tooth. The forces exerted on each side of the blank tooth form its morphology. The change of the frictional force's direction exerted on the driven side can lead to the inconsistent ear shape on the two sides of the tooth top.

### 4.2 Deformation analysis

Figure 8 shows the effective strain diagram of the blank when the gear roller feeds 0.75 mm. It may be seen in this figure that the strains are mainly distributed on the surface of the teeth sides and on the teeth roots, where the metal material is compressed, while no deformation occurs in the inner region of the teeth. This is because, in the gear rolling process, the tooth of the gear roller and the tooth of the blank maintain a generating motion relation. The relation makes the tooth surface of the blank and the tooth surface of the gear roller keep continuous local contact, resulting in the material on the tooth surface plastic yield in sequence. The material on the tooth surface of the blank is constrained by the axial undeformed zone at both ends; it thus flows radially towards the direction of the smaller resistance, that is, the direction along the flank of the tooth.

### 4.3 Flow analysis

Figure 9 shows the continuous velocity vector diagram of the blank while the gear roller, spinning counterclockwise, is forming tooth C. Tooth A first extrudes the tooth root located on the right side of tooth C. The metal nearby moves towards the upper-left along the contact surface between the tooth flank of the blank and that of the gear roller. This leads to the tooth wider and taller, as shown in Fig. 9a. The gear roller continues to roll to form the tooth. When tooth B of the gear roller contacts the active side of the blank, the metal nearby is squeezed, and it flows along the left side of the tooth towards the tooth top of the blank. Simultaneously, the metal on the

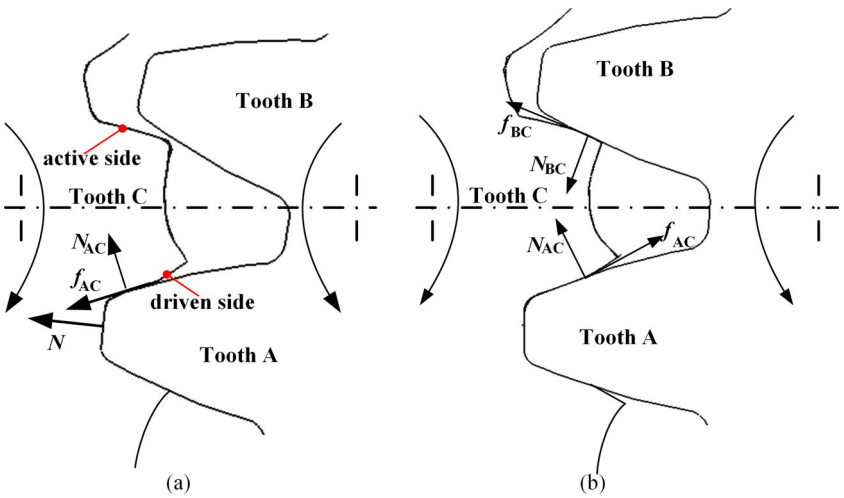


**Fig. 7** Force analysis in the gear rolling process. **a** Tooth *A* rolls tooth *C*. **b** Teeth *A* and *B* roll tooth *C*

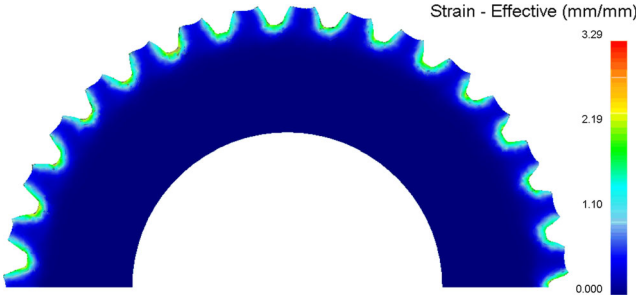


**Fig. 8** Effective strain distribution of the blank in gear rolling

driven side of tooth C continues to be squeezed by the gear roller. In this course, tooth C is squeezed by teeth A and B. Thus, the metal flows towards the direction of the smaller resistance. That is the direction along the flank towards the tooth top. The deformation is concentrated in the surface of the tooth side. For the metal on the surface of the tooth side, the distance from the side of the tooth to the side of the tooth top is shorter than the side of the tooth to the center of the tooth top. In addition, the flow resistance is smaller correspondingly. Therefore, more metal flows along the flank to the tooth top, and the metal of the two sides on the tooth top protrudes to form the rabbit ear, as shown in Fig. 9b. As the gear roller continues to roll the blank, tooth A gradually slides out, and tooth B is gradually slides in. The squeezing pressure exerted on the active side of tooth C becomes greater than the driven side, and the metal on the active side of tooth C is therefore pressed to flow towards the upper-right direction, which causes the concave of the tooth top not be centered but rather center right, as shown in Fig. 9c. In the final step of the rolling process, tooth B begins to contact and extrudes the next tooth root of the blank. At the same time, tooth A gradually slides out of the last tooth root. In the course, tooth A continues to keep partial contact with the driven side of the blank. Tooth A exerts extrusion and pulls on the driven side of the blank. Thus, the ear on the driven side of the tooth top is pulled up and turns sharp, as shown in Fig. 9d.

In the following section, a velocity analysis is presented, employing the point tracking method of evenly distributed locations at the tooth top. The objective of this analysis is to bring further insight into the formation of the ear rabbit defect.

When the gear roller feeds 0.75 mm and extrudes one tooth, five points are carefully selected along the surface of the tooth top, as shown in Fig. 10a. The velocity curves of these five points, obtained from the point tracking method, are displayed in Fig.10b. It may be seen in this figure that the speeds of all five points reach two peak values in the examined timeframe. The first maximum value of each point's velocity curve appears when the gear roller contacts and rolls the right side of the blank, and the speed difference between the five points is not significant, and the difference between maximum and minimum is about 10%. Then, when the next tooth of the gear roller contacts and rolls the left side of this tooth, the speeds of the points $P_1$ to $P_4$ reach the maximum value successively, with a magnitude of $V_{P1} > V_{P2} > V_{P3} > V_{P4}$. As for the point $P_5$, located at the right edge of the tooth top, when the last tooth of the gear roller slides out, the metal nearby $P_5$ is pulled up, which causes the speed of the point $P_5$ to reach its second maximum value. Furthermore, it may be seen from these velocity curves that the average velocity of the points $P_1$, $P_2$, and $P_5$, located near the edges of the tooth top, is larger than that of the points $P_3$ and $P_4$, which are located on the center of the tooth top. The average speed of the point $P_4$ is in fact the smallest of all five, which shows that the metal flow on the right center of the tooth top is the slowest, resulting in the most concave area, thus corroborating the result of the flow analysis above.

From the stress state, the distribution of deformation and the flow condition, it is known that the surface metal compressed flows towards the flank of the tooth, and the velocity difference induces metal protrude on the two sides of the tooth top. The rabbit ear forms. The asymmetry of the rabbit ear is relevant with the different direction of the friction exerted on the two sides of the tooth, related to the rotation direction of

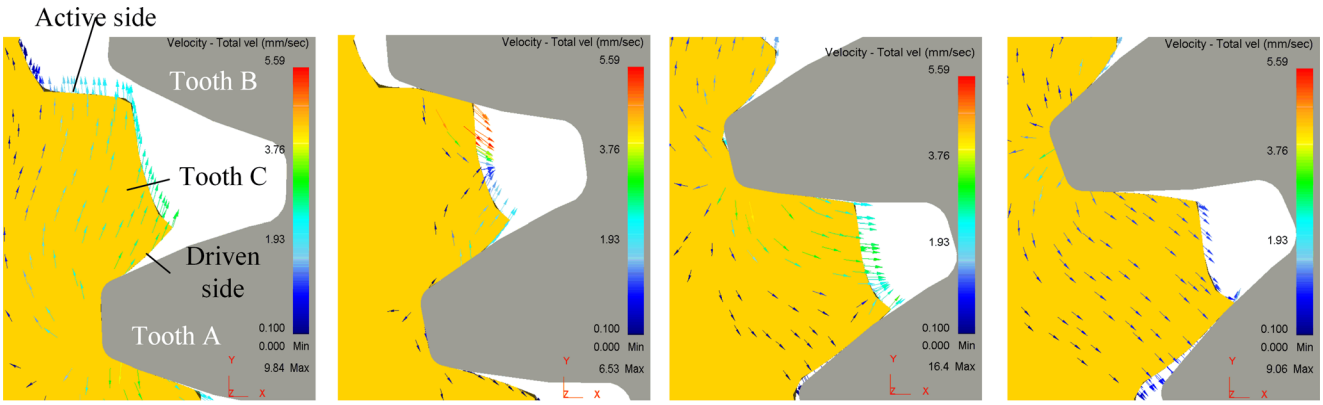


**Fig. 9** Continuous velocity vector diagram while the gear roller rolling a tooth of the blank. **a** Initial phase. **b** Middle phase. **c** Last phase. **d** Finish

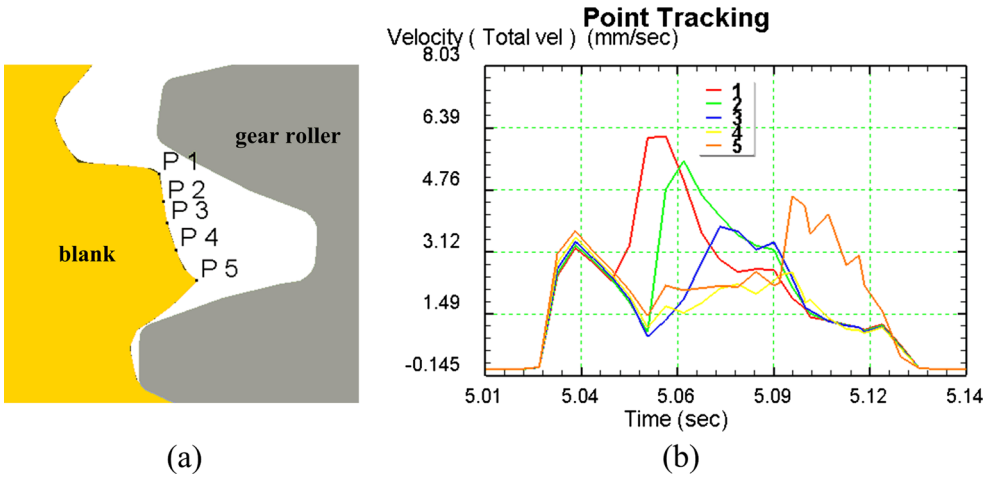


**Fig. 10** Velocity of points tracking. **a** Position distribution of tracking points. **b** Velocity curve of tracking points

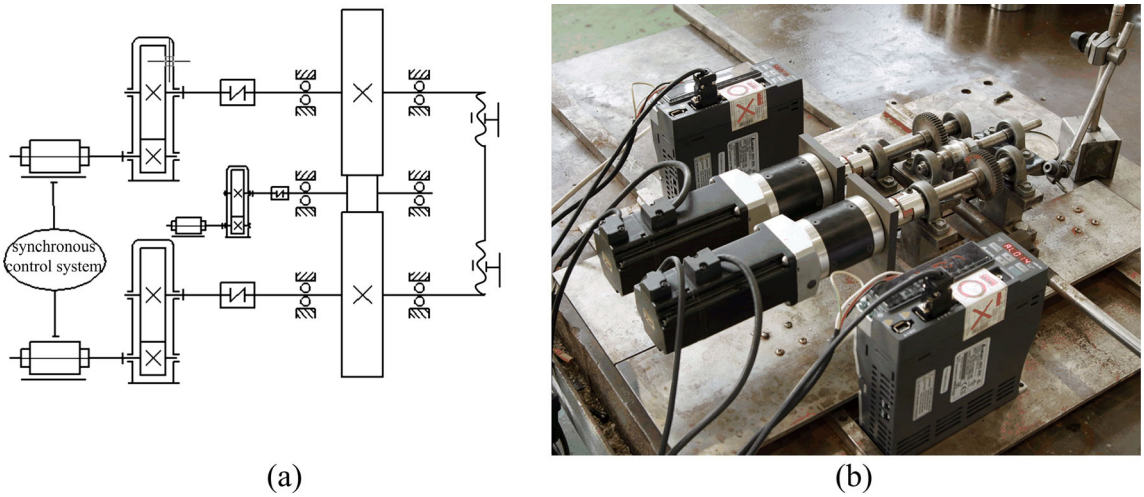


**Fig. 11** Gear rolling device. **a** Device schematic diagram. **b** Experimental apparatus

the gear roller. As shown in Fig.7b, teeth *A* and *B* of the gear roller conform tooth *C* of the blank. The direction of friction on the active side of tooth *A* and that on the driven side of tooth *A* is different. When tooth *A* slides out from tooth *C*, the material on the contact surface (that is the driven side) is pulled outwards; thus, the rabbit ear on the driven side turns sharp and tall. The rabbit ear is a typical defect in gear rolling, which is caused by the special generating motion between the gear roller and the blank.

## 5 Experimental verification and analysis of results

According to the principle of gear rolling process, a set of double gear roller experimental setup was designed and manufactured, as shown in Fig. 11. The blank material was selected as AL_2017 softened by annealing process for 24 h; the blank was made as a step along the radial direction, and the outer margin thickness of the blank was 2 mm, as shown in Fig.12. The rolling process was conducted under the same conditions than those employed for the numerical simulations. The two gear rollers both feed 1.00 mm along the radial axis, and the morphology of the tooth of the gear to be formed is shown in Fig. 13. It may be seen in the photos how protrusions clearly appear on both sides of the tooth top with an asymmetric shape: one is tall and sharp while the other is short and stout. Based on the rotational direction of the gear roller, it

**Fig. 12** The AL_2017 blank with a radial step

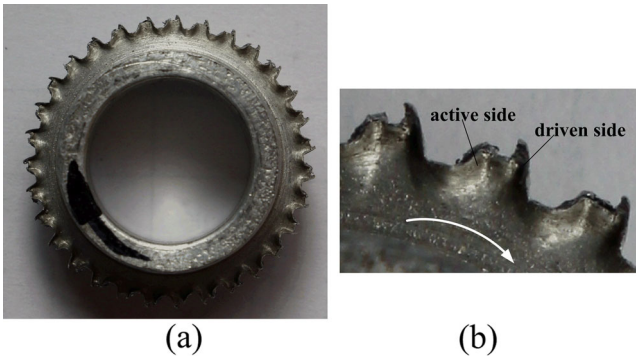


**Fig. 13** Morphology of the rabbit ear in the experiment. **a** The gear rolled. **b** Enlarged view of the rabbit ear

may be deduced that the tall and sharp protrusion is located on the driven side while the short and stout protrusion lies on the active side. Meanwhile, the teeth bend counterclockwise. Because the feed is smaller, the bending phenomenon is not very obvious. The morphology of teeth in the simulation is shown in Fig. 14, while the feed of the gear rollers is 1.00 mm. The comparison between Figs. 13 and 14 shows that morphology of the rabbit ear and the bending of the teeth in experiment are consistent with those in simulation.

## 6 Conclusions

In this paper, a numerical model of gear rolling process was established in accordance to a motion relationship between the gear roller and the blank. The gear rolling forming was thus simulated. The morphological changes of the rabbit ear was presented, and the formation mechanism of the rabbit ear was studied through the analysis of the stress state, the deformation distribution, and the metal flow.

1. In the gear rolling process, with the feed increase of the gear roller, the tooth gradually grows taller and the rabbit ear defect appears. The two ears are asymmetric because the ear on the driven side of the tooth is pulled up and turns sharp. With further formation of the tooth, the ears on both sides appear to combine and fold.
2. The gear roller and the blank maintain a continuous localized contact because of their generating motion, which cause the material in the surface region of the blank yield sequential plastic deformations. At the same time, the material squeezed by the tooth flank of the gear roller, flows towards the direction of the smaller resistance, that is, the flank of the tooth, which causes the flow velocity difference of the material between on the two sides and on the center of the tooth top, resulting in the formation of the rabbit ear.
3. The asymmetry of the ears appears to be related to the direction of friction exerted on the two sides of the blank tooth depending on the rotational direction of the gear roller. The ear on the driven side is pulled up, along the flank of tooth, by the sliding-out tooth of the gear roller.
4. In order to validate these numerical findings, an experimental setup of a double gear roller was designed and manufactured. The rolling process was then conducted under the same conditions than those employed for the numerical simulations. The morphology of the rabbit ear and the bending of the teeth formed during the experiment were consistent with the simulation results.

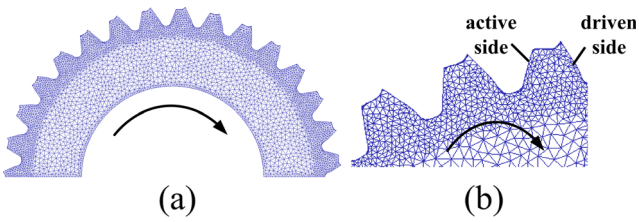


**Fig. 14** Morphology of the rabbit ear in the simulation. **a** The gear rolled. **b** Enlarged view of the rabbit ear

**Acknowledgements** This project was supported by the National Natural Science Foundation of China (Grant No. 51475271).

## References

1. Kondo K, Ohga K (1995) Precision cold die forging of a ring gear by divided flow method. International Journal of Machine Tools & Manufacture 35:1105–1113
2. Choi JC, Choi Y (1999) Precision forging of spur gears with inside relief. Int J Mach Tools Manuf 39:1575–1588
3. Hu CL, Liu QK, Zhao Z, Chen J, Wu GM (2010) Two step forging process of spur gear based on rigid parallel motion. Journal of Shanghai Jiaotong University(Science) 15:241–244
4. Jung SY, Kang MC, Kim C, Kim CH, Chang YJ, Han SM (2009) A study on the extrusion by a two-step process for manufacturing helical gear. Int J Adv Manuf Technol 41:684–693
5. Li J, Wang GC, Wu T (2016) Numerical simulation and experimental study of slippage in gear rolling. J Mater Process Technol 234: 280–289
6. Zheng WG, Chen D (2005) The situation of studying on technologies of rolling plasticity forming for gears. Journal of plasticity engineering 12:43–46
7. Liu ZQ(2012) Theoretical and experimental study on cold rolling precision forming of spline shafts. Lanzhou University of Technology
8. Sun YZ (2011) Virtual design and numerical analysis on cylindrical gear rolling process. Wuhan University of Technology
9. Wu WH (2004) The processing problem of involute spline rolling. Machinist Metal Cutting 26–26
10. Wang JL, Jin ZY, Liu SQ (2014) Dimension calculation of diameter before rolling for small modulus involute spline by cold roll forming. Journal of Mechanical Transmission 38:167–171
11. Zhu XX, Wang BY, Yang LY, Zuo B, Li Z (2014) Effect of relative sliding on tooth profiles metal flow during gear roll forming. J Univ Sci Technol Beijing 36:246–251
12. Wang GC, Li J (2015) A gear rolling forming method for improving the rabbit ear defect. Patent. China. CN104438993A

13. Kamouneh AA, Ni J, Stephenson D, Vriesen R, DeGrace G (2007) Diagnosis of involute metric issues in flat rolling of external helical gears through the use of finite-element models. Int J Mach Tools Manuf 47:1257–1262
14. Neugebauer R, Hellfritzsch U, Lahl M (2008) Advanced process limits by rolling of helical gears. International Journal of Material Forming Suppl 01:1183–1186
15. Neugebauer R, Putz M, Hellfritzsch U (2007) Improved process design and quality for gear manufacturing with flat and round rolling. CIRP Annals-Manufacturing Technology 56:307–312
16. Neugebauer R, Klug D, Hellfritzsch U (2007) Description of the interactions during gear rolling as a basis for a method for the prognosis of the attainable quality parameters. Prod Eng 01:253–257
17. Nagata E, Kurita N (2011) Form rolling method for involute gear. Patent. Japan. CN 102294419 A
18. Sasaki H, Shinbutsu T, Amano S, Takemasu T, Sugimoto S, Koide T, Nishid S (2014) Three-dimensional complex tooth profile generated by surface rolling of sintered steel helical gears using special CNC form rolling machine. Procedia Engineering 81:316–321
19. Uematsu S (2002) Effect of variation of angular velocity in gear rolling process on profile error. Journal of the Japan Society for Precision Engineering 26:425–429
20. Yu QH, Liu SM, Liu YH (2015) Technology optimization of hot forging crankshaft based on DEFORM 3D. Hot Working Technology 44:132–134